Climate change impacts on glaciers and water resources in the headwaters of the Tarim River, NW China/Kyrgyzstan

Michel Wortmann[1,*], Doris Duethmann[2,3], Christoph Menz[1], Tobias Bolch[5], Shaochun Huang[1,5], Jiang Tong[6], Zbigniew W. Kundzewicz[1,7] and Valentina Krysanova[1]

[1] Potsdam Institute for Climate Impact Research, Telegrafenberg A31, 14473 Potsdam, Germany

[2] German Research Center for Geosciences, Telegrafenberg, 14473 Potsdam, Germany

[3] IGB Leibniz Institute of Freshwater Ecology and Inland Fisheries Berlin, Müggelseedamm 310, 12587 Berlin, Germany

[4] Geography & Sustainable Development, University of St Andrews, North Street, St Andrews KY16 9AL, United Kingdom

[5] Norwegian Water Resources and Energy Directorate (NVE), PO Box 5091, Majorstua, 0301 Oslo, Norway

[6] National Climate Centre, Chinese Meteorological Administration, No. 46, Zhongguancun South Street, Beijing, China

[7] Institute for Agricultural and Forest Environment of the Polish Academy of Sciences, Bukowska 19, 60-809 Poznań, Poland

* Corresponding author (wortmann@pik-potsdam.de)

Abstract

Glacierised river catchments have been shown to be highly sensitive to climate change, while large populations may depend on their water resources. The irrigation agriculture and the communities around the Tarim River, NW China, are strongly dependent on the discharge from the highly glacierised catchments surrounding the Taklamakan Desert. While recent increasing headwater discharge has been beneficial for the expanding agricultural sector, future runoff under climate change is uncertain. We assess three climate change scenarios (Representative Concentration Pathways (RCP) 2.6, 4.5, 8.5) by forcing two glacio-hydrological models with output of eight General Circulation Models. The models have different glaciological modelling approaches but were both calibrated to discharge and glacier mass balance observations. Projected changes of temperature, precipitation, glacier cover and river discharge are examined over the 21st century and generally point to a warmer and wetter climate in the ensemble median. The climate model ensemble projects median temperature and precipitation increases of +1.9–5.3°C and +9–24%, respectively, until the end of the century compared to 1971–2000. Glacier area is projected to shrink by 15–73% (model medians, range over scenarios), strongly depending on catchment and scenario. River discharge is projected to first increase by about

20% in the Aksu River catchments with subsequent decreases of up to 20% until 2100 compared to 1971–2000. In contrast, discharge in the drier Hotan and Yarkant catchments is projected to increase by 15–60% towards the end of the century. The large uncertainties mainly relate to climate model ensemble and the limited observations to constrain the glacio-hydrological models.

Keywords

Tarim River, SWIM-G, WASA, climate change impact assessment, glacio-hydrological modelling

Funding

This study was conducted within the project SuMaRiO (Sustainable Management of River Oases along the Tarim River; http://www.sumario.de/), funded by the German Federal Ministry of Education and Research (BMBF grants 01LL0918J, 01LL0918I and 01LL0918B). T. Bolch acknowledges funding by Deutsche Forschungsgemeinschaft (DFG, BO3199/2-1).

Conflicts of interest

None declared.

Availability of code and data

Upon reasonable request.

Authors' contributions

M.W., D.D. and V.K. designed the study. M.W. performed the SWIM-G simulations and drafted the manuscript. D.D. carried out the WASA simulations and contributed to the draft. C.M. processed and analysed the climate input data. T.B. provided the glacier input and validation data. S.H., J.T. and Z.K. were involved in data acquisition and research design. All authors contributed to the final version of the manuscript.

---

1. Introduction

The Tarim River in the Xinjiang Uighur Autonomous Region of NW China is the country's largest endorheic river basin and is home to approx. 10 Million people. Runoff is generated in the glacierised Tien Shan (Aksu River), Pamir, Karakoram (Yarkant R.) and Kunlun Mountains (Hotan R.) encircling the Taklamakan Desert and is vital to the linear river oases that live from

irrigation agriculture. A decline in upstream runoff may have severe consequences for the population, agriculture and ecosystems downstream, threatening the very existence of the river as it has done in the past (Thevs, 2011). As most mountainous regions, the highly glacierised and largely uninhabited headwaters of the Tarim River are vulnerable to climate change, as higher temperatures endanger the glaciers as natural reservoirs for downstream communities (Barnett et al., 2005; Immerzeel et al., 2020; Pritchard 2019). At the same time, competition for river water has dramatically increased over the past 30 years with the rapid expansion of irrigated agriculture for the production of cotton, fruit and subsistence farming. While an increase in headwater discharge has been observed (Liu et al., 2006; Krysanova et al., 2015), downstream discharge has declined in line with a four-fold increase in irrigation area over the past 40 years (Thevs, 2011).

The continental climate produces scarce precipitation mainly in summer when it coincides with the glacier melt peak (Aizen et al., 1995). Meteorological measurements are sparse and mainly in valleys or at the fringes of the Taklamakan Desert (Tao et al., 2011; Krysanova et al., 2015), which introduces an underestimation in catchment-wide precipitation interpolations. Comparing various datasets and using glacio-hydrological modelling, Wortmann et al. (2018) show that the best available dataset (APHRODITE, Yatagai et al., 2012) has to be corrected by factors of 1.2–4.3 at the catchment average (more at higher elevations) to be consistent with discharge records and glacier mass balances estimates. Similar findings are reported for other areas in the Tarim basin and its surroundings (Duethmann et al., 2013; Immerzeel et al., 2015; Tong et al., 2014).

Several studies about the Tarim River basin investigate the observed trends in discharge and its anticipated climatic (Xu et al., 2004; Chen et al., 2006; Liu et al., 2006; Yaning et al., 2009, Li et al.,2020), as well as water management drivers (Song et al., 2002; Liu and Chen, 2006; Tang et al., 2007; Hao et al., 2008; Wu et al., 2010). A small number of contributions have addressed changes of glaciers or glacier runoff under projected climate change, but only at a regional scale (Kraaijenbrink et al., 2017; Huss and Hock, 2018; Rounce et al., 2020) or in parts of the Tarim Basin. Duethmann et al. (2016) examine three climate change scenarios in the Aksu headwaters and project glacier area to decrease by 32-90% over the 21st century with an initial increase and an eventual decrease in discharge. Zhang et al. (2012) assess glacier runoff, mass balance and area over the first half of the 21st century using a simple degree-day glacier melt model and three delta-change scenarios. However, no systematic assessment of future changes under common climate change scenarios, considering the extensive glacier cover and their

heterogenous response to climate change in the headwaters, has been conducted to date. This is largely because of a complex hydrology and the data scarcity or restrictions on the limited data availability.

Assessments of glacier area and mass balance in the Tarim headwaters are crucial for adequate hydrological modelling. Recent advances have been made; for example, different glacier inventories exist covering large parts (2nd Chinese glacier inventory, Guo et al., 2015) or the whole basin (the Randolph Glacier Inventory consisting of different sources, RGI consortium, 2017). Investigations of observed glaciological changes at the catchment scale have been conducted for the Aksu headwaters by Pieczonka and Bolch (2015), using multitemporal satellite images and digital terrain models. Although the existing mass balance assessments for the Yarkant and Hotan catchments only cover shorter periods (Brun et al., 2017; Shean et al., 2020) or not the entire catchment area (Holzer et al., 2015; Zhou et al., 2018), they still provide evidence for the calibration of glacio-hydrological models.

This study aims to provide a first systematic climate change impact assessment for the 21st century of the Tarim River headwaters simulating glacier and hydrologic changes based on two glacio-hydrological models (SWIM-G and WASA). The use of an ensemble of global circulation model (GCM) results as well as two hydrological models is meant to expose the inherent uncertainty associated with both sources. Huang et al. (2018), uses the projected discharge and considers the water management in the river oases downstream under the same climate change scenarios.

2. Study region: The Tarim River headwaters

The Tarim River is one of the largest endorheic rivers in the world with a topographical catchment size of about 800,000 km^2 and a mainstream length of 600–800 km depending on discharge and water abstractions (Tao et al., 2011). The river is fed by three large tributaries with their confluence at the northern edge of the Taklamakan Desert: The Aksu River originating in the central Tien Shan to the north, the Hotan River originating in the Kunlun Shan to the south and the Yarkant River originating in eastern Pamir and the Karakoram (see Figure 1). The desert climate in the lower parts of these rivers and the Tarim produces virtually no river runoff (except for rare extreme rain events) with annual potential evapotranspiration exceeding precipitation by a factor of 30–50 (Zhao et al., 2012). The vast majority of river discharge is generated in the mountainous and glacierised headwaters. This study focuses on the five catchments of the gauging stations that are situated at the boundary of the Taklamakan

129 Desert, i.e. before significant river abstractions and transmission losses occur (Table 1 and
130 Figure 1).

131 **Table 1** Catchment statistics for all considered stations with annual and June-August mean
132 discharge (Q, 1961-1989, with some gaps), glacier cover of 2008 (Pieczonka and
133 Bolch, 2015; Duethmann et al., 2016), mean annual precipitation (P, 1971-2000) of the
134 APHRODITE dataset (Yatagai et al., 2012) and corrected median values of precipitation Pc by
135 Wortmann et al. (2018). Precipitation estimates (95% uncertainty range) by Duethmann et al.
136 (2015) are given for the Aksu catchments as footnotes.

137 **Figure 1** Map of the five considered catchments (their names marked by a white shade) that
138 supply the vast majority of discharge to the Tarim River. Wortmann et al., 2018 © American
139 Meteorological Society. Used with permission.

140 The climate of the headwaters is highly continental with a strong seasonality governed by the
141 Westerlies, with parts of the Hotan and Yarkant catchment also influenced by the Indian
142 monsoon (Aizen et al., 1995; Maussion et al., 2014). As a consequence, river regimes exhibit a
143 strong peak in summer when snow and glacier melt coincide with the precipitation peak. Mean
144 summer (winter) temperatures fall between 3–20°C (-19– -5°C) with about 75% of precipitation
145 falling between the months of April and September.

146 The mountain ranges surrounding the Taklamakan Desert comprise steep, high-altitude terrain
147 that has given rise to an extensive glacier cover accounting for significant proportions of the
148 catchment areas considered here (Figure 1, Table 1). The two Aksu headwaters comprise a total
149 glacier area of 3410±118 km^2 (2008, Pieczonka and Bolch, 2015; Osmonov et al., 2013). A
150 unique glaciological feature of the Aksu headwaters is the ice-dammed Merzbacher Lake that
151 sends near-annually recurring subglacial outburst floods (jökulhlaups) downstream with
152 consequences for communities and modelling efforts (Glazirin, 2010; Wortmann et al., 2014).
153 The two catchments of the Hotan River span the north-western edge of the Tibetan Plateau and
154 have a glacier cover of some 5880 km^2 (Shangguan et al., 2007). The Yarkant headwater has a
155 total glacier cover of about 5600 km^2 at extremely high and steep altitudes (Dyurgerov, 2010).

156 Observed signs of a changing climate in the headwaters have been widely discussed. An
157 increasing trend in river discharge over the past 50 years of the Aksu River, the most important
158 tributary to the Tarim River, was reported to be as much as 30% between 1957 and 2004
159 relative to mean discharge (Wang et al., 2008; Krysanova et al., 2015). This was attributable to
160 increasing trends in air temperature and precipitation, with a higher contribution of air
161 temperature in the Xiehela catchment, as found by a modelling and data-based study

(Duethmann et al., 2015). An increasing trend could, however, not be confirmed for the discharge of the Hotan and Yarkant catchments (Tao et al., 2011). The observed climate in Xinjiang has experienced a trend towards warmer and wetter conditions since the 1970s (Shi et al., 2006). Statistically significant increasing trends were found for temperature, precipitation and vapour pressure over nearly the entire Tarim catchment (at 1% significance level, Tao et al., 2011). Due to the poor observation density in the Hotan and Yarkant headwaters, however, those results must be interpreted with caution. Long-term, high-altitude observations for these catchments do not exist, rendering the hydrological observations the only long-term glimpse of these catchments' water balance and even those are interrupted.

Glaciological studies in the Tarim are also rare, but the Aksu catchment has again received most research, especially over the last decade. Pieczonka and Bolch (2015) have recently found a heterogeneous glacier mass and area loss over the catchment, but the average mass balance of 0.35±0.34 m weq. a^{-1} (1970–2008) is comparable to global values. Other studies have confirmed and contributed to this assessment (Farinotti et al., 2015; Pieczonka et al., 2013; Osmonov et al., 2013). Investigations in the Karakoram based on declassified satellite imagery from the 1970s indicate stable conditions or only slight mass loss: Bolch et al. (2017) found a mass balance of -0.01±0.09 m weq. a^{-1} (1973--1999) for the Hunza catchment and Zhou et al. (2017) found a mass balance of -0.04±0.05 m weq. a^{-1} (1973–2000) for the central Karakoram. However, both studies focus on the part draining southwards into the Indus. Studies of mass changes since 2000 show a positive or stable balance in the Tarim part of the Karakoram, the Kunlun Mountains, and eastern Pamir, e.g. +0.04±0.05 m weq. a^{-1} (2000–2018, Shean et al., 2020), +0.05±0.07 m weq. a^{-1} (2003–2008, Kääb et al., 2015) and +0.14±0.08 (2000–2016, Brun et al., 2017).

3. Data and Methods

This climate change impact assessment considers future hydrological and glaciological changes by assessing multiple scenarios and climate model results by means of two glacio-hydrological models. SWIM-G (Wortmann et al., 2019) and WASA (Güntner, 2002) models were implemented in the five headwater catchments, calibrated and validated to discharge and glacier observations and then driven by results of eight GCMs. What has become a common practice of climate impact assessment in many river catchments of the world (Fowler et al., 2007; Beniston, 2003; Teutschbein and Seibert, 2012) is a task marred with difficulties in the complex hydrology of the Tarim River; the stark contrast between desert and mountain climate,

194 severe data scarcity, heterogenous past glacier changes (Shean et al., 2020), substantial river
195 abstractions downstream (Tao et al., 2011) and regular large glacial lake outbursts (Wortmann
196 et al., 2014) to name but a few. The validated models were then run with climate scenarios over
197 the reference period and the 21st century. The reference or baseline period is defined as 1971–
198 2000 and three future periods are investigated, i.e. the near (2011–40), medium (2041–70) and
199 far (2071–2100) future.

200 **3.1. Input data**

201 To overcome the precarious data availability, mostly preprocessed (homogenised, synthesised)
202 datasets are used in this study (Table 2). They offer best-practice interpolations of the sparse
203 observations (homogenised also beyond national boundaries), while also circumventing
204 restrictive data sharing policies of China. Precipitation is the most crucial driving variable and
205 the renown APHRODITE dataset (Yatagai et al., 2012), a gridded precipitation interpolation of
206 the densest gauge network in Asia, was used. Although it is the best data available, the station
207 density is still extremely poor. E.g. the Hotan and Yarkant catchments are nearly devoid of any
208 observations with the closest stations located at the edge of the Taklamakan Desert or at
209 significantly lower-laying locations (Tao et al., 2011, Wortmann et al., 2018) leading to a
210 negative bias. The necessary precipitation correction used according to Duethmann et al. (2013,
211 WASA) and Wortmann et al. (2018, SWIM-G) is shortly described in the next section.

212 Other driving data include temperature (daily mean, minimum, maximum), radiation and
213 relative humidity, which are provided by the WATCH Forcing Data (v2) (Weedon et al., 2011).
214 Although it suffers from the same or worse station sparsity as the APHRODITE data, the
215 climate variables are significantly more stable over space and time. The variability of
216 temperature with elevation (lapse rate) is also more stable – especially in dry climates – and is
217 therefore parameterised in the snow and glacier melt components of the models.

218 **Table 2** Input data used to drive and calibrate/validate the models. Topography and glaciers are
219 shown in Fig. 1. Climate variables are: temperature T (mean, min., max.), precipitation P,
220 radiation and relative humidity.

221 **3.2. Glacio-hydrological modelling**

222 **3.2.1. SWIM-G**

223 The glacio-hydrological model SWIM-G is used to simulate both glacier and the catchment
224 hydrology in a tightly integrated approach (Wortmann et al., 2019; 2018). It was developed
225 from the widely applied and tested semi-distributed ecohydrological model SWIM (Krysanova

et al., 1998) that was recently extended by a glacier dynamics module and was especially developed for long-term climate change impact assessments for medium to large river basins. Krysanova et al. (2015) provides an overview of the hydrological processes considered. The glacier dynamics extension includes all important glacier processes at the glacier scale, including ice flow, avalanching, sublimation and debris evolution (see Annex 1.1 for a brief description and Wortmann et al., 2019). It was developed to overcome the conflict of scale between individual glaciers and the catchment hydrology when modelling larger, highly glacierised, typically data-scarce catchments. It relies on computational units that disaggregate complex terrain into parts of similar elevation, aspect and hydrological subbasin as opposed to gridded (fully distributed) or empirical approaches (e.g. Immerzeel et al., 2011; Huss et al., 2010). They are conceptually similar and computationally equal to the hydrological response units (HRUs) implemented in SWIM, enabling a tight integration between glaciological and hydrological modelling over large catchments.

The model was calibrated and validated in the period 1961–1987 as in-situ observations were available, using a multi-objective Pareto optimisation with three objective functions (calibration ensemble median ranges in parentheses): 1) to the observed discharge at the five outlet gauge stations using a combined Nash-Sutcliffe efficiency (0.73–0.94) and the root mean square error of mean annual discharge as objective functions (13–21%), 2) to observed glacier area using the hypsometry matching metric X^2 as objective function (8-15%) and 3) to mass balances using an error probability function (0.001–0.023). The calibration also includes the initialisation of the glacier cover by running the glacier dynamics driven by the climate of 1960-1975 repeatedly over 300 years to yield a glacier cover and thickness adapted to both the driving data and the model structure. The model initialisation and calibration is described in more detail in Wortmann et al. (2018) and the median performance values are given in Table A1 (Annex 1.2). For the Hotan and Yarkant catchments, long-term mass balance measurements were not available and the most plausible scenario was chosen instead. The model calibration yielded several 'non-dominated' parameter sets, all of which are considered equally valid. The parameter set that offers the best trade-off between all objective functions was chosen for the scenario runs presented in the results (see description and Figure A2 in Annex 1.3). For an uncertainty assessment, the scenarios were also run with the best/worst parameter sets and an analysis of variance (ANOVA, Gottschalk, 2006) was conducted, comparing the variance between climate model ensemble, scenario and parameter set (Figure A8 in Annex 2).

3.2.2. WASA

WASA is a semi-distributed, process-based hydrological model. It was first applied to semiarid catchments in Brazil (Güntner, 2002; Güntner and Bronstert, 2004) and Spain (Francke et al., 2008; Mueller et al., 2010) and more recently to snow and glacier dominated high mountain catchments in Central Asia (Duethmann et al., 2013; 2014; 2015). Detailed model descriptions including equations can be found in Güntner and Bronstert (2004) and Duethmann et al. (2015) with a brief description provided in Annex 1.4.

The present study uses a daily time step and the spatial structure is organized based on catchments, subcatchments and 200 m elevation zones. For calculating glacier area and volume changes, glaciers are considered individually and a finer discretization of 50 m elevation bands is used. The initial glacier ice thickness distribution of each glacier was derived from a spatially distributed ice-thickness model (GlabTop2) (Linsbauer *et al* 2012, Frey *et al* 2014). Based on the simulated mass balance of the glacier, thickness changes in each elevation band are calculated using predefined functions derived from observed glacier thickness changes of the Ak-Shirak massif in the period 1977-1999 (Surazakov and Aizen, 2006). For the Hotan and Yarkant catchments, the model was calibrated to daily discharge data over a 10-year calibration period from 1979 to 1988. The period 1972-1978 was used for model evaluation. Additional two-year periods were used for model initialization. Glacier mass balances for this region were not available for the period 1979-1988. It was assumed that glacier mass balances for the Hotan and Yarkant basins during the calibration period were close to balance, and the mass loss was constrained to 0±0.1 m w.eq. a^{-1} (Bolch et al., 2017; Shean et al., 2020). For the Aksu catchment, the model was calibrated in a multi-objective way using daily discharge variations, interannual variations of seasonal discharge, discharge trends, correlation to the observed annual glacier mass balance series and cumulative glacier mass change based on geodetic estimates (Duethmann et al., 2015). The calibration period was defined from 1976-1999 and the periods 1957-1975 and 2000-2004 were used for model evaluation. From the set of Pareto optimal solutions, one solution was selected for further evaluations in this study. For details of the WASA model calibration in the Aksu catchment, please refer to Duethmann et al. (2015). Daily calibration (validation) Nash-Sutcliffe Efficiency ranged between 0.60–0.85 (0.71–0.84). All performance results of the calibration are provided in Table A2 (Annex 1.4).

3.3. Climate change scenarios

We use three well established scenarios from the IPCC Representative Concentration Pathways (RCP; IPCC, 2014): a) RCP 2.6 (atmospheric greenhouse gas concentration peaking around 2040 at 490 ppm CO_2-eq and eventual decline), b) RCP 4.5 (stabilisation at 650 ppm CO_2-eq at

the end of the 21st century) and c) RCP 8.5 (continuous rise above 1370 ppm CO_2-eq after 2100). The results of eight GCMs from the from the coupled model intercomparison project phase 5 (CMIP5) were used (Table A3 in Annex 1.6, Taylor et al., 2012). The models were selected to cover the full range of precipitation and temperature change signals from the CMIP5 ensemble over the Tarim headwater catchments, i.e. the moderate and strong cases of wetter-warmer, wetter-colder, drier-warmer, drier-colder signals. The GCMs have spatial resolutions ranging from 1.5–3° and all data was provided at a daily temporal resolution.

GCM results were bias-adjusted relative to the baseline period 1971–2000 to the original driving data that the glacio-hydrological models were calibrated to (Wang et al., 2013, Duethmann et al., 2016). A non-parametric quantile mapping approach with trend preservation was chosen, as was previously used by Hempel et al. (2013). Despite concerns of the validity of using a bias-adjustment for climate change impact assessments (Ehret et al., 2012), it was considered necessary in the Tarim headwaters because of considerable deviations in precipitation between calibration and scenario driving data as well as the great sensitivity of the glacier cover to even slight differences in climatic conditions. The application was paramount to ensure plausible reference conditions for the ensemble assessment.

4. Results

4.1. Changes in temperature and precipitation

Increases in both temperature and precipitation are projected under most climate scenarios, with significant changes in all headwater catchments relative to the reference period 1971–2000 (Figure 2 for annual and period changes, Figures A4-A5 in the Annex for monthly regimes of all periods and catchments). All ensemble median values in the three projection periods increase across all regions. Only ensemble minimum signals indicate possible negative changes in precipitation, especially in the Aksu. Strong increases in (median) temperature and precipitation from the reference period to the near future are projected (often stronger than changes in subsequent periods).

Temperature increases are similar across all regions. In the near future, they range between 0.5°C and 2.4°C with only small differences between the scenarios. Those differences become more striking in the two later periods, when ensemble median changes increase with RCP scenario. In the medium-term future, they peak for the RCP 2.6 scenario at about 2.5°C and slightly decrease thereafter, while for the higher RCP scenarios they continue to increase up to 7°C (ensemble max.) in the far future for RCP 8.5. The ensemble variability generally increases

with time, leading to ranges of about 2–4°C in the far future. As expected, snowfall is more confined to the winter months, as time and emission scenario progresses (Figure A6 for monthly snow fractions in the Annex).

Changes in precipitation are less uniform across regions and projection periods and exhibit an even greater ensemble variability, a pattern common in other regions (Thompson et al., 2013; Vetter et al., 2013). Relative changes in the near future are modest and similar across the regions and scenarios with median values of about 6–8%. Scenario differences become more pronounced in the two later periods, as ensemble median changes vary with RCP scenario (with the exception of the medium term in the Aksu catchment). Changes in the Aksu catchment range from decreases of up to 25% to increases of the same magnitude, but the majority of models indicate increases in precipitation with median changes of 11–18%. These increases are similar in the Hotan and Yarkant catchments, but the spread is large and mostly positive (-15 to +54%).

Figure 2 Climate change scenarios for the Tarim headwaters for the 21st century, including the reference period (1971–2000). Ensemble maximum, median and minimum values are shown as 10-year running means and signals averaged over the near (2011-40), medium (2041-70) and far (2071-2100) future. Absolute values are given in the left vertical axis and changes relative to the reference period along the right axis. Note that these are bias-adjusted GCM results without the static precipitation bias correction applied by the glacio-hydrological models. Monthly regimes for all periods, scenarios and catchments are provided in Figure A4-A5 in the Annex.

4.2. Changes in glacier area and volume

A receding trend over the 21st century is evident in all catchments for the ensemble medians of both models and it is strengthening with RCP scenario (Fig. 3, period mean changes in Table A4 in the Annex). For the ensemble medians, glaciers are projected to shrink by up to 35% in the near future, 2–64% in the medium future and 8–89% in the far future compared to the reference period across the three scenarios. and large ranges are due to differences between two impact models and RCP scenarios. In the Xiehela and Shaliguilanke (Aksu) catchments, area shrinkage for the high-end RCP 8.5 scenario steadily rises to 55-80% and 80-95% by the end of the century, respectively, compared to 2010. Both lower scenarios show lower levels of 32–49% and 51–74%, respectively (Figure 3).

Figure 3 Simulated glacier area changes relative to mean area in the reference period (1971-2000) over the reference and scenario periods for the three RCP scenarios and the five catchments (indicated by their outlet station and main Tarim headwater river). Median values are computed over the climate model ensemble. Period mean values including ensemble standard deviations are provided in Table A4 in the Annex.

For the SWIM-G projections, median shrinkages are highest for Shaliguilanke (Aksu) and lowest for Tongguziluoke (Hotan) catchment. Glacier changes in this highly glacierised catchment are similar to those in the Xiehela (Aksu) catchment (both with a catchment glacier cover ≈ 20%), i.e. reaching about -50% until 2100 under RCP8.5. The long-term changes of the less glacierised Wuluwati (Hotan) and Kaqun (Yarkant) catchments are similar to the Shaliguilanke (Aksu) catchment (7, 12 and 5% glacier cover, respectively), i.e. close to -75% under RCP8.5. Differences between the lower two scenarios, however, are larger in the Hotan and Yarkant catchments than in the Aksu, and they show a slower recession in the first half of the century.

The median shrinkages of the WASA projections are also highest for Shaliguilanke and lowest for Tongguziluoke. Both Wuluwati and Kaqun show lower levels than Xiehela (all periods) but higher than Tongguziluoke (from the mid-century). In the near future period, practically no changes are projected for the Yarkant and Hotan. The changes for the end of the century are also highest for Shaliguilanke (reaching almost -100% under RCP8.5), and lowest for Tongguziluoke (>-25%). The final changes by the end of the century are similar for Xiehela and Kaqun (reaching ca. -75% at RCP8.5), and moderate at Wuluwati.

Comparing projections between two impact models, it is evident that WASA simulates much stronger decline of glacier areas in the Aksu basin than SWIM-G from the mid-century. However, SWIM-G generates higher losses than WASA in the Hotan and Yarkant catchments, though by the end of the century both models come to similar results for the Kaqun station (Yarkant).

In line with area changes, glacier volume (in water equivalents) is also projected to decrease under all scenarios (Table A4, Figure A6 in the Annex). Projected mass loss is 4–25% in the near, 12–75% in the medium and 18–97% in the far future across all catchments and scenarios for the ensemble median. Losses are consistently the greatest in the Shaliguilanke (Aksu) catchment, lower in the Xiehela (Aksu), Wuluwati (Hotan) and Kaqun (Yarkant) catchments, and they are the lowest in the Tongguziluoke (Hotan) catchment.

Glacier mass balances give an indication of the glacier imbalance, the hydrological impact thereof and they may be better compared to studies of past glacier evolution. Decadal mean annual mass balances are provided in Figure A7 (Annex). The glacier recession described above is associated with negative mass balances that maintain or exceed the negative rates of the past in the first half of the 21st century with a recovery for the RCP 2.6 and 4.5 scenarios

391 and an acceleration for the RCP 8.5 by the end of the century. The near future (2011–2040)
392 shows similar mass balances to those observed in the past across the region – about -0.4–0 m
393 weq. a^{-1} – with little differences between scenarios. The largest negative mass balances for the
394 two lower-end scenarios are projected for the middle of the century, while they continue to
395 grow more negative in the high-end scenario until they reach -1.2–-0.8 m weq. a^{-1} by the end of
396 the century. A recovery to stable or even positive mass balances is only projected under the
397 RCP 2.6 and 4.5 scenarios in the far future analogues to the temperature projections (Fig. 2).

398 **4.3. Changes in river discharge**

399 The discharge results of the multi-model analysis are summarised in Figure 4 for each
400 catchment and period. In the two Aksu subcatchments, the increase in mean annual discharge is
401 most pronounced in the near future but recedes in subsequent periods except for the RCP 8.5
402 scenario simulated by SWIM-G in the Xiehela catchment. The initial increase is 10 to 25% for
403 the ensemble median relative to the 1971–2000 reference period (higher values from WASA
404 compared to SWIM-G) with a slight increase relative to the RCP forcing. In the medium and
405 long term, the increase in the Aksu catchment reduces progressively and turns to no or negative
406 changes compared to the reference period, especially under the RCP 2.6 scenario in the Xiehela
407 catchment and under the RCP 8.5 scenario in the Shaliguilanke catchment.

408 The impacts are different in the Hotan and Yarkant catchments. There is a general trend of
409 increasing mean annual discharge apparent at all stations and nearly all time periods. Changes
410 in mean annual discharge in these catchments show a uniformly increasing trend at greater
411 magnitudes as in the Aksu catchment. The initial increase in the near future is around 25 to
412 40% (ensemble median). Subsequent periods also show increases, especially under RCP 8.5.
413 The RCP 4.5 simulations peak in the medium term at 28–60% compared to the baseline period,
414 while the RCP 2.6 scenario shows lower or similar increases in the later periods than in the
415 first.

416 **Figure 4** Projected future changes in annual mean discharge simulated by SWIM-G and
417 WASA. Changes are relative to the baseline period 1971–2000.

418 The changes in discharge are predominantly concentrated in the summer months (Figure 5).
419 April to June discharge predominantly increases in the Aksu catchments for all scenarios
420 (mostly higher increase according to WASA), July–September discharge tends to increase in
421 the near future but decreases in the far future. The Hotan and Yarkant catchments show
422 increases in the summer months (June to September) that progress with period and RCP

scenario. Discharge only decreases under the RCP 2.6 and RCP 4.5 scenarios in August-September in the Yarkant in the far future. Winter discharge changes in all catchments are mostly positive but represent only small fractions of the increase in the annual discharge. Changes in discharge according to SWIM-G are mostly lower than WASA in the Aksu catchment but higher in the Hotan and Yarkant.

Figure 5 Absolute regime changes in the three main headwaters of the Tarim River (sum of both headwaters in the Aksu and Hotan). The ensemble median is shown for each scenario and glacio-hydrological model. Rather than relative changes for each month in comparison with the reference period, the absolute monthly changes are shown to account for the highly seasonal flows.

The origin of these changes can be traced by investigating the changes in the runoff generating water inputs, i.e. rain, glacier and snow melt (Figure 6). As would be expected under warmer and wetter climate conditions, the rain is increasing in all catchments under most scenarios and the glacier melt is mostly decreasing. An exception is the highly glacierised Tongguziluoke (Hotan) catchment, where both rain and glacier melt are increasing, indicating an increased redistribution of ice into the ablation zone and explaining the sharp projected increases in discharge. The snowmelt is nearly constant or slightly increasing, except in the Shaliguilanke (Aksu) catchment according to WASA under the RCP 8.5 scenario. The changes in discharge components reveal the peak in glacier melt predominantly in the first half of the 21st century for the Hotan and Yarkant catchments (Figure 6). Under the RCP 8.5 scenario the peak is shifted further into the second half of the century, which is especially evident in the Tongguziluoke (Hotan) catchment.

Figure 6 Projected glacier melt, snow melt and rain (absolute input values in mm a^{-1} distributed over the catchment areas). 10-year running mean values of the ensemble median for both SWIM-G and WASA are shown.

5. Discussion

Results indicate a marked increase in river discharge, which is in-line with observations over the past decades (Tao et al., 2011; Li et al., 2020). Given the arid climate combined with the vast ice reserves, higher temperatures leading to negative glacier mass balances are able to drastically change river discharge in the short and medium term until ‘peak meltwater’ is reached (Sorg et al., 2012, Huss and Hock, 2018). The two existing studies estimate the peak of the glacier meltwater to be reached at about 2030 in the low emission scenario and about 2060 or 2070 in the high emission scenario for whole Tarim basin (Huss and Hock, 2018; Rounce et

al., 2020). Our study showed that these projected peaks for the whole basin can mainly be attributed to the Asku basin as Hotan and Yarkand show distinct different behaviour. The peak water seems to be in sight under all scenarios in the Aksu catchments as both glacio-hydrological models indicated the largest increases in the near future (Fig. 4, 5). In the Hotan and Yarkant catchments, this peak is only evident in the medium to far future mainly under the low and moderate emissions scenarios. Projected significant increases in precipitation are also driving the strong increases in discharge and are able to compensate for melt water losses. However, precipitation is quite variable from year to year while glacier melt is a more reliable water source (Bolch, 2017; Pritchard, 2019). Moreover, precipitation projections are subject to high uncertainties.

The use of two glacio-hydrological models with different representations and processes of glaciers allows a more robust understanding of model uncertainties. Both models generally agree on the direction of glacial and discharge changes with the exception of discharge in the Aksu catchment in the far future, where ensemble ranges point in both directions but the medians disagree. Disagreements in change magnitude are most evident in the glacier recession in the Aksu (WASA greater reductions) and the Hotan catchments (SWIM-G greater reduction) with WASA indicating a stronger increase in discharge in the short and medium term in the Xiehela catchment and SWIM-G predicting slightly stronger median increases in the Hotan catchments. Ensemble ranges of discharge changes (Fig. 4) are generally greater for WASA with some exceptions in the Tongguziluoke catchment. Water balance components (Fig. 6) also show some strong differences, as WASA generally shows higher values of rain and snow melt and SWIM-G larger values of glacier melt in the Hotan and Yarkant catchments. The differences between the glacio-hydrological models is predominantly caused by different assumptions in the precipitation correction, a key calibration term and uncertainty in these catchments (cf. P in Table 1), as well as by differences in the calculation of evapotranspiration. SWIM-G simulates lower rates of rain and snowmelt and in the Hotan and Yarkant catchments in the first half of the 21st century also higher rates of glacier melt, since WASA assumes a stronger precipitation correction. While the uncertainties between the two models with respect to precipitation correction appear large, these are actually small when compared to the precipitation estimates based on observation products or to simulated precipitation by GCMs. Thus, glacio-hydrological modelling in combination with observed discharge and glacier mass balances or glacier area distribution can be a suitable alternative to derive precipitation estimates. An ensemble of glacio-hydrological models is useful to assess the uncertainties of

such precipitation estimates.

The differences in flow components may explain some of the differences in the changes in annual discharge. Higher contribution of rain makes WASA more susceptible to the higher ensemble variability in precipitation leading to greater uncertainty ranges. Higher shares of glacier melt in SWIM-G in the Tongguziluoke catchment lead to greater sensitivity to temperature increases, producing greater increases in discharge. Differences in glacial changes are likely attributable to the different representations of ice in the models. For example, the glacier recession in WASA is steeper in the first half of the 21st century in the Aksu catchments leading to a pronounced glacier melt peak, while SWIM-G produces more gradual changes. This may be caused by the different approaches for calculating glacier area and volume changes, and processes that are considered by the SWIM-G model but not by the WASA model, such as glacier dynamics, sublimation and debris accumulation (Wortmann et al., 2019).

Model parameter uncertainty was quantified using the calibration and climate change scenario ensemble via an analysis of variance (for SWIM-G in Figure A5 in the Annex and for WASA in Duethmann et al. (2016) Figure 4). For discharge, the variance related to different parameter sets amounts to less than 20% of the total, while the differences related to the climate model ensemble makes up more than 50%. For the initialised glacier area (SWIM-G only), model parameters explain more than 80% of the variance in the reference period and at the beginning of the scenario period, as the initialised glacier area depends largely on mean temperature and precipitation which are both bias-adjusted. This changes rapidly though over the course of the 21st century, when the GCM ensemble again explains more than 70% of the variance. Reductions in the different sources of uncertainties will ultimately only come from better observations to further constrain parameter ranges and improve modelled process representations (Bolch et al., 2012). For example, high elevation precipitation measurements could help constrain the precipitation correction and help improve estimates of elevation-dependent warming (MRIEDWWG, 2015) or stable isotope measurements could reveal the share of runoff from rain, snow and glacier melt (Kumar et al., 2011; Ohlanders et al., 2013; He et al., 2019). Lastly, improvements in the GCM projections would likely have the largest impact on uncertainties in the glacier and discharge projections presented here, as the use of a GCM ensemble has shown. This study may serve as a justification for future investments in the improvement of these broader deficiencies.

6. Conclusions

This study represents the first systematic and comprehensive climate change impact assessment of the Tarim River headwater catchments for the 21st century, using state-of-the-art GCM climate projections and scenarios as well as two large-scale, glacio-hydrological models. Together, changes in these catchments will largely determine the water resources of the Tarim River and the communities living in and around the Taklamakan Desert in the Xinjiang Uighur Autonomous Region. The assessment is the product of significant research efforts to simulate the complex water resources of these remote and largely ungauged mountain ranges. It required the construction of two large-scale glacio-hydrological models (Wortmann et al., 2019; Duethmann et al., 2016) and the correction of precipitation datasets as well as the subsequent model calibration under data-scarce conditions (Wortmann et al., 2018; Duethmann et al, 2013). These efforts have enabled a robust impact assessment based not only on a single impact model but two that can expose the model-inherent uncertainties.

In line with regional and global trends, results indicate a warmer and wetter climate with substantial consequences for the high-mountain glacier cover and the meltwater-driven rivers. Depending on the low, medium or high emission scenarios, temperatures are projected to rise by about 1.9°C, 3.2°C or 5.3°C in the ensemble mean by the end of this century (2071-2100) compared to the 1971-2000 reference period, while precipitation may intensify by about 9%, 14% or 24%. The two calibrated and specifically adapted glacio-hydrological models, SWIM-G and WASA, project these climatic changes to result in a shrinkage of the glacier cover by around 45%, 52% or 73% (median of both models and catchments) in the Aksu headwaters and by about 21%, 28% or 40% in the Hotan and Yarkant headwaters for the low, medium or high emissions scenarios, respectively. Similarly, the models project river discharge to mainly increase in the Hotan and Yarkant catchments by the end of the century (by about 15%, 30% or 60%), while in the Aksu headwater it is projected to first increase (by about 20% regardless of scenario) to return to or even decrease below reference discharge by the end of the century. Discharge increases are greatest in the spring and summer months (April–September) and decreases in the Aksu catchment mainly occur in August–September due the diminished glacier meltwater.

Despite the shrinking glacier cover, precipitation increases drive the changes in river discharge and at least partially compensate the losses in meltwater. The receding trend in the Aksu headwaters is important, however, as the Aksu headwaters currently dominate the discharge of

553 the Tarim River. With the projected increases in the Hotan and Yarkant headwaters, this could
554 change, depending on the agricultural water abstractions in the river oases lining these
555 tributaries (Huang et al. 2018). Future research should focus on reducing the large uncertainties
556 that remain in the simulation of glacio-hydrological changes in this region that are mainly
557 driven by the climate ensemble, the glacio-hydrological models and the limited observations
558 available for constraining the models during the historical period.

559

560

References

Aizen, V., E. Aizen, J. Melack, 1995. Climate, snow cover, glaciers, and runoff in the Tien Shan, Central Asia. JAWRA Journal of the American Water Resources Association, 31(6):1113–1129.

Barnett, T. P., J. C. Adam, D. P. Lettenmaier 2005. Potential impacts of a warming climate on water availability in snow-dominated regions. Nature, 438(7066):303–309.

Beniston, M. 2003. Climatic Change in Mountain Regions: A Review of Possible Impacts. In Climate Variability and Change in High Elevation Regions: Past, Present & Future, H. F. Diaz, ed., number 15 in Advances in Global Change Research, Pp. 5–31. Springer Netherlands.

Beniston, M. 2006. Mountain Weather and Climate: A General Overview and a Focus on Climatic Change in the Alps. Hydrobiologia, 562(1):3–16.

Bolch, T., 2017. Asian glaciers are a reliable water source. Nature 545, 161-162.

Bolch, T., Kulkarni, A., Kääb et al., 2012. The State and Fate of Himalayan Glaciers. Science 336, 310–314.

Bolch, T., Pieczonka, T., Mukherjee, K., Shea, J., 2017. Brief communication: Glaciers in the Hunza catchment (Karakoram) have been nearly in balance since the 1970s. The Cryosphere 11, 531–539.

Bolch, T., Shea, J.M., Liu, S. et al., 2019. Status and Change of the Cryosphere in the Extended Hindu Kush Himalaya Region, in: Wester, P., Mishra, A., Mukherji, A., Shrestha, A.B. (Eds.), The Hindu Kush Himalaya Assessment: Mountains, Climate Change, Sustainability and People. Springer International Publishing, Cham, pp. 209–255.

Brun, F., Berthier, E., Wagnon, P. et al., 2017. A spatially resolved estimate of High Mountain Asia glacier mass balances from 2000 to 2016. Nature Geoscience 10, 668–673.

Chen, Y., K. Takeuchi, C. Xu et al., 2006. Regional climate change and its effects on river runoff in the Tarim Basin, China. Hydrological Processes, 20(10):2207–2216.

Duethmann, D., J. Zimmer, A. Gafurov et al., 2013. Evaluation of areal precipitation estimates based on downscaled reanalysis and station data by hydrological modelling, HESS, 17, 2415-2434.

Duethmann, D., Peters, J., Blume, T. et al., 2014. The value of satellite-derived snow cover images for calibrating a hydrological model in snow-dominated catchments in Central Asia, Water Resour. Res., 50, 2002-2021.

Duethmann, D., T. Bolch, D. Farinotti et al., 2015. Attribution of streamflow trends in snow- and glacier melt dominated catchments of the Tarim River, Central Asia. Water Resources Research, Pp. 4727–4750.

Duethmann, D., C. Menz, T. Jiang, S. Vorogushyn 2016. Projections for headwater catchments of the Tarim River reveal glacier retreat and decreasing surface water availability but uncertainties are large. Environmental Research Letters, 11(5).

Dyurgerov, M. B. 2010. Reanalysis of Glacier Changes: From the IGY to the IPY, 1960-2008, number 108 in Data of Glaciological Studies. Moscow: Glaciological Association, Geographical Institute of the Russian Academy of Sciences.

Ehret, U., E. Zehe, V. Wulfmeyer et al., 2012. HESS Opinions ”Should we apply bias correction to global and regional climate model data?”. Hydrology and Earth System Sciences; Katlenburg-Lindau, 16(9):3391.

FAO, IIASA, ISRIC et al., 2011. The Harmonized World Soil Database. Database 1.2, FAO and IIASA, Rome.

Farinotti, D., L. Longuevergne, G. Moholdt et al., 2015. Substantial glacier mass loss in the Tien Shan over the past 50 years. Nature Geoscience, 8(9):716–722.

Fowler, H. J., S. Blenkinsop, C. Tebaldi 2007. Linking climate change modelling to impacts studies: Recent advances in downscaling techniques for hydrological modelling. International Journal of Climatology, 27(12):1547–1578.

Frey H, Machguth H, Huss M, Huggel C, Bajracharya S, Bolch T, Kulkarni A, Linsbauer A, Salzmann N and Stoffel M 2014 Estimating the volume of glaciers in the Himalayan–Karakoram region using different methods. The Cryosphere 8 2313-33

Friedl, M. A., D. K. McIver, J. C. F. Hodges et al., 2002. Global land cover mapping from MODIS: Algorithms and early results. Remote Sensing of Environment, 83(1-2):287–302.

Glazirin, G. 2010. A century of investigations on outbursts of the ice-dammed Lake Merzbacher (Central Tien Shan). Austrian Journal of Earth Sciences, 103(2):171–179.

Gottschalk, L., 2006. Methods of Analyzing Variability, in: Encyclopedia of Hydrological Sciences. John Wiley & Sons, Ltd.

Hao, X., Y. Chen, C. Xu, and W. Li 2008. Impacts of Climate Change and Human Activities on the Surface Runoff in the Tarim River Basin over the Last Fifty Years. Water Resources Management, 22(9):1159–1171.

He, Z., Unger-Shayesteh, K., Vorogushyn, S. et al., 2019. Constraining hydrological model parameters using water isotopic compositions in a glacierized basin, Central Asia, J. Hydrol., 571, 332-348.

Hempel, S., K. Frieler, L. Warszawski et al., 2013. A trend-preserving bias correction; the ISI-MIP approach. Earth System Dynamics, 4(2):219–236.

Huang, S., F. F. Hattermann, V. Krysanova, A. Bronstert 2013. Projections of climate change impacts on river flood conditions in Germany by combining three different RCMs with a regional eco-hydrological model. Climatic Change, 116(3-4):631–663.

Huang, S., V. Krysanova, H. Österle, F. F. Hattermann 2010. Simulation of spatiotemporal dynamics of water fluxes in Germany under climate change. Hydrological Processes, 24(23):3289–3306.

Huang, X., H. Xie, T. Liang, D. Yi 2011. Estimating vertical error of SRTM and map-based DEMs using ICESat altimetry data in the eastern Tibetan Plateau. International Journal of Remote Sensing, 32(18):5177–5196.

Huang, S., Wortmann, M., Duethmann, D. et al., 2018. Adaptation strategies of agriculture and water management to climate change in the Upper Tarim River basin, NW China. Agricultural Water Management 203, 207–224.

Huss, M., Hock, R., 2018. Global-scale hydrological response to future glacier mass loss. Nature Climate Change 8 (2), 135–140.

Huss, M., Jouvet, G., Farinotti, D., and Bauder, A. (2010). Future high-mountain hydrology: A new parameterization of glacier retreat, Hydrol. Earth Syst. Sci., 14, 815-829.

Immerzeel, W.W., F. Pellicciotti, A.B. Shrestha 2012. Glaciers as a Proxy to Quantify the Spatial Distribution of Precipitation in the Hunza Basin. Mountain Research and Development, 32(1):30–38. 00023.

Immerzeel, W.W., L.P.H. van Beek, M. Konz et al., 2011. Hydrological response to climate change in a glacierized catchment in the Himalayas. Climatic Change, 110(3-4):721–736.

Immerzeel, W.W., A. Lutz, M. Andrade et al., 2020. Importance and vulnerability of the world's water towers. Nature 577, 364–369.

IPCC 2007. IPCC Fourth Assessment Report: Climate Change 2007 (AR4). 00389.

IPCC 2014. Summary for Policymakers. In Climate Change 2014: Impacts, Adaptation, and Vulnerability. Part A: Global and Sectoral Aspects. Contribution of Working Group II to the Fifth Assessment Report of the Intergovernmental Panel on Climate Change, C. B. Field et al., eds., Pp. 1–32. Cambridge, United Kingdom, and New York, NY, USA: Cambridge University Press.

Jarvis, A., H. Reuter, A. Nelson, and E. Guevara 2007. Hole-filled seamless SRTM data, version 4. DEM, International Centre for Tropical Agriculture (CIAT).

Kraaijenbrink, P.D.A., Bierkens, M.F.P., Lutz, A.F., Immerzeel, W.W., 2017. Impact of a global temperature rise of 1.5 degrees Celsius on Asia's glaciers. Nature 549, 257–260.

Krysanova, V., D. Müller-Wohlfeil, and A. Becker 1998. Development and test of a spatially distributed hydrological/water quality model for mesoscale watersheds. Ecological Modelling, 106(2-3):261–289.

Krysanova, V., M. Wortmann, T. Bolch et al., 2015. Analysis of current trends in climate parameters, river discharge and glaciers in the Aksu River basin (Central Asia). Hydrological Sciences Journal, 60(4):566–590.

Kumar, B., 2011. Isotopic Characteristics of Ice, Snow, and Glaciers, in: Singh, V.P., Singh, P., Haritashya, U.K. (Eds.), Encyclopedia of Snow, Ice and Glaciers, Encyclopedia of Earth Sciences Series. Springer Netherlands, pp. 665–668.

Li, Z., Shi, X., Tang, Q., Zhang, Y. et al., 2020. Partitioning the contributions of glacier melt and precipitation to the 1971–2010 runoff increases in a headwater basin of the Tarim River. Journal of Hydrology 583, 124579.

Linsbauer A, Paul F and Haeberli W 2012 Modeling glacier thickness distribution and bed topography over entire mountain ranges with GlabTop: Application of a fast and robust approach. Journal of Geophysical Research-Earth Surface 117 F03007.

Liu, S., Y. Ding, D. Shangguan et al., 2006. Glacier retreat as a result of climate warming and increased precipitation in the Tarim river basin, northwest China. Annals of Glaciology, 43(1):91–96.

Liu, Y. and Y. Chen 2006. Impact of population growth and land-use change on water resources and ecosystems of the arid Tarim River Basin in Western China. International Journal of Sustainable Development & World Ecology, 13(4):295–305.

Maussion, F., D. Scherer, T. Mölg et al., 2014. Precipitation Seasonality and Variability over the Tibetan Plateau as Resolved by the High Asia Reanalysis. Journal of Climate, 27(5):1910–1927.

MRIEDWWG, 2015. Elevation-dependent warming in mountain regions of the world. Nature Clim. Change 5, 424–430.

Ohlanders, N., Rodriguez, M., McPhee, J., 2013. Stable water isotope variation in a Central Andean watershed dominated by glacier and snowmelt. Hydrol. Earth Syst. Sci. 17, 1035–1050.

Osmonov, A., T. Bolch, C. Xi, A. Kurban, and W. Guo 2013. Glacier characteristics and changes in the Sary-Jaz River Basin (Central Tien Shan, Kyrgyzstan) – 1990–2010. Remote Sensing Letters, 4(8):725–734.

Pieczonka, T. and T. Bolch 2015. Region-wide glacier mass budgets and area changes for the Central Tien Shan between ˜ 1975 and 1999 using Hexagon KH-9 imagery. Global and Planetary Change, 128:1–13.

Pieczonka, T., T. Bolch, W. Junfeng, and S. Liu 2013. Heterogeneous mass loss of glaciers in the Aksu-Tarim Catchment (Central Tien Shan) revealed by 1976 KH-9 Hexagon and 2009 SPOT-5 stereo imagery. Remote Sensing of Environment, 130:233–244.

Pritchard, H.D., 2019. Asia's shrinking glaciers protect large populations from drought stress. Nature 569, 649–654.

RGI Consortium (2017). Randolph Glacier Inventory – A Dataset of Global Glacier Outlines: Version 6.0: Technical Report, Global Land Ice Measurements from Space, Colorado, USA. Digital Media.

Rounce, D.R., Hock, R., Shean, D.E., 2020. Glacier mass change in High Mountain Asia through 2100 using the open-source python glacier evolution model (PyGEM). Frontiers in Earth Science 7, 331.

Shangguan, D., L. Shiyin, D. Yongjian et al., 2007. Glacier changes in the west Kunlun Shan from 1970 to 2001 derived from Landsat TM/ETM+ and Chinese glacier inventory data. Annals of Glaciology, 46(1):204–208.

Shean, D.E., Bhushan, S., Montesano et al., 2020. A Systematic, Regional Assessment of High Mountain Asia Glacier Mass Balance. Front. Earth Sci. 7.

Shi, X. Z., D. S. Yu, E. D. Warner et al., 2004. Soil Database of 1:1,000,000 Digital Soil Survey and Reference System of the Chinese Genetic Soil Classification System. Soil Horizons, 45(4):129.

Shi, Y., Y. Shen, E. Kang et al., 2006. Recent and Future Climate Change in Northwest China. Climatic Change, 80(3-4):379–393.

Shi, Y., Liu, C., Kang, E., 2009. The Glacier Inventory of China. Annals of Glaciology 50, 1–4.

Song, Y., R. Wang, and Y. Peng 2002. Water resources and ecological conditions in the Tarim Basin. Science in China Series D: Earth Sciences, 45:11–17.

Sorg, A., M. Huss, M. Rohrer, and M. Stoffel 2014. The days of plenty might soon be over in glacierized Central Asian catchments. Environmental Research Letters, 9(10):104018.

Tang, Q., H. Hu, T. Oki, and F. Tian 2007. Water Balance within Intensively Cultivated Alluvial Plain in an Arid Environment. Water Resources Management, 21(10):1703–1715.

Tao, H., M. Gemmer, Y. Bai et al., 2011. Trends of streamflow in the Tarim River Basin during the past 50 years: Human impact or climate change? Journal of Hydrology, 400(1-2):1–9.

Taylor, K.E., R.J. Stouffer, G.A. Meehl, 2012, An overview of CMIP5 and the experiment design, Bull. Amer. Meteor. Soc., 93, 485-498.

Teutschbein, C. and J. Seibert 2012. Bias correction of regional climate model simulations for hydrological climate-change impact studies: Review and evaluation of different methods. Journal of Hydrology, 456–457:12–29.

Thevs, N. 2011. Water Scarcity and Allocation in the Tarim Basin: Decision Structures and Adaptations on the Local Level. Journal of Current Chinese Affairs, 40(3):113–137.

Thompson, J. R., A. J. Green, D. G. Kingston et al., 2013. Assessment of uncertainty in river flow projections for the Mekong River using multiple GCMs and hydrological models. Journal of Hydrology, 486:1–30.

Vetter, T., S. Huang, V. Aich et al., 2015. Multi-model climate impact assessment and intercomparison for three large-scale river basins on three continents. Earth Syst. Dynam., 6(1):17–43.

Vetter, T., S. Huang, T. Yang et al., 2013. Intercomparison of climate impacts and evaluation of uncertainties from different sources using three regional hydrological models for three river basins on three continents. In Proceedings of the IMPACTS World Conference.

Wang, D., C. Menz, T. Simon et al., 2013. Regional dynamical downscaling with CCLM over East Asia. Meteorology and Atmospheric Physics, 121(1-2):39–53.

Wang, G., Y. Shen, H. Su et al., 2008. Runoff Changes in Aksu River Basin during 1956-2006 and Their Impacts on Water Availability for Tarim River. Journal of Glaciology and Geocryology, 30(4):562–568.

Wang, Y., ed. 2006. Local records of the Aksu River basin. Beijing, China: Fangshi Publisher.

Weedon, G. P., S. Gomes, P. Viterbo et al., 2011. Creation of the WATCH Forcing Data and Its Use to Assess Global and Regional Reference Crop Evaporation over Land during the Twentieth Century. Journal of Hydrometeorology, 12(5):823–848.

Wortmann, M., V. Krysanova, Z. W. Kundzewicz et al., 2014. Assessing the influence of the Merzbacher Lake outburst floods on discharge using the hydrological model SWIM in the Aksu headwaters, Kyrgyzstan/NW China. Hydrological Processes, 28(26):6337–6350.

Wortmann, M., Bolch, T., Menz, C. et al., 2018. Comparison and Correction of High-Mountain Precipitation Data Based on Glacio-Hydrological Modeling in the Tarim River Headwaters (High Asia). J. Hydrometeor. 19, 777–801.

Wortmann, M., Bolch, T., Su, B., Krysanova, V., 2019. An efficient representation of glacier dynamics in a semi-distributed hydrological model to bridge glacier and river catchment scales. Journal of Hydrology 573, 136–152.

Wu, Z., H. Zhang, C. Krause, and N. Cobb 2010. Climate change and human activities: A case study in Xinjiang, China. Climatic Change, 99(3):457–472.

Xu, H., B. Zhou, Y. Song 2010. Impacts of climate change on headstream runoff in the Tarim River Basin. Hydrology Research, 42(1):20.

Xu, Z. X., Y. N. Chen, J. Y. Li 2004. Impact of Climate Change on Water Resources in the Tarim River Basin. Water Resources Management, 18(5):439–458.

Yaning, C., X. Changchun, H. Xingming et al., 2009. Fifty-year climate change and its effect on annual runoff in the Tarim River Basin, China. Quaternary International, 208(1–2):53–61.

Yatagai, A., K. Kamiguchi, O. Arakawa et al., 2012. APHRODITE: Constructing a Long-Term Daily Gridded Precipitation Dataset for Asia Based on a Dense Network of Rain Gauges. Bulletin of the American Meteorological Society, 93(9):1401–1415.

Zhang, X., D. Yang, X. Xiang, X. Huang, 2012. Impact of agricultural development on variation in surface runoff in arid regions: A case of the Aksu River Basin. Journal of Arid Land, 4(4):399–410.

Zhang, Y., S. Liu, Y. Ding 2006. Observed degree-day factors and their spatial variation on glaciers in western China. Annals of Glaciology, 43(1):301–306.

Zhao, C., Shi, F., et al., 2012. The tendency and influencing factors of surface water evaporation in Aksu Oasis in recent 30 years.

Zhou, Y., Li, Z., Li, J. et al., 2018. Glacier mass balance in the Qinghai–Tibet Plateau and its surroundings from the mid-1970s to 2000 based on Hexagon KH-9 and SRTM DEMs. Remote Sensing of Environment 210, 96–112.

Tables and figures

Table 1 Catchment statistics for all considered stations with station elevation, annual and June-August mean discharge (Q, 1961-1989, with some gaps), glacier cover of 2008 (Pieczonka and Bolch, 2015; Duethmann et al., 2016), mean annual precipitation (P, 1971-2000) of the APHRODITE dataset (Yatagai et al., 2012), corrected median values of precipitation Ps by Wortmann et al. (2018), used in SWIM-G, and corrected values of precipitation Pw estimated based on observed discharge and glacio-hydrological modelling with WASA.

River (Tarim trib.)	Station	Area	St. elev.	Q	JJA Q	Glacier	P	Ps	Pw
		km^2	m a.s.l.	$m^3 s^{-1}$	$m^3 s^{-1}$	%	$mm\ a^{-1}$	$mm\ a^{-1}$	$mm\ a^{-1}$
Kumarik (Aksu)	Xiehela	12 989	1472	146.7	406.6	19.8	314	487	526
Toshkan (Aksu)	Shaliguilanke	18 408	1924	84.4	208.1	4.3	230	327	387
Karakash (Hotan)	Wuluwati	20 600	1874	71.4	200.5	12.2	98	230	285
Yurungkash (Hotan)	Tongguziluoke	14 890	1629	71.1	223.3	23.0	62	285	302
Yarkant (Yarkant)	Kaqun	46 759	1451	208.9	578.7	12.3	113	267	320

Table 2 Input data used to drive and calibrate/validate the models. Topography and glaciers are shown in Fig. 1. Climate variables are: temperature T (mean, min., max.), precipitation P, radiation and relative humidity.

Data	**Source**
Climate	WATCH (Weedon et al., 2011) for temperature (mean, min., max.), radiation and relative humidity
	AHPRODITE (Yatagai et al., 2012) for precipitation* Interpolated station data (used for the WASA model in the Aksu catchment)
Topography	SRTM hole-filled digital elevation model at 90 m resolution (Jarvis et al., 2007)
Land cover	China Meteorological Administration, MODIS 500 m land cover (2001) (Friedl et al., 2002)
Soil	Harmonised World Soil Database (FAO et al., 2011), includes the $1:10^6$ soil map for China (Shi et al., 2004)
Glaciers	Outlines from generated by Pieczonka and Bolch (2015) and Osmonov et al. (2013) and GlabTop simulated thickness (Duethmann et al., 2015; Paul and Linsbauer, 2012) for model initialisation/calibration
Discharge	Daily river discharge at 5 gauges from Chinese hydrological yearbooks for the period 1964-87 (with some gaps) for model calibration

* correction and catchment-specific variations are described in Section 2.3.

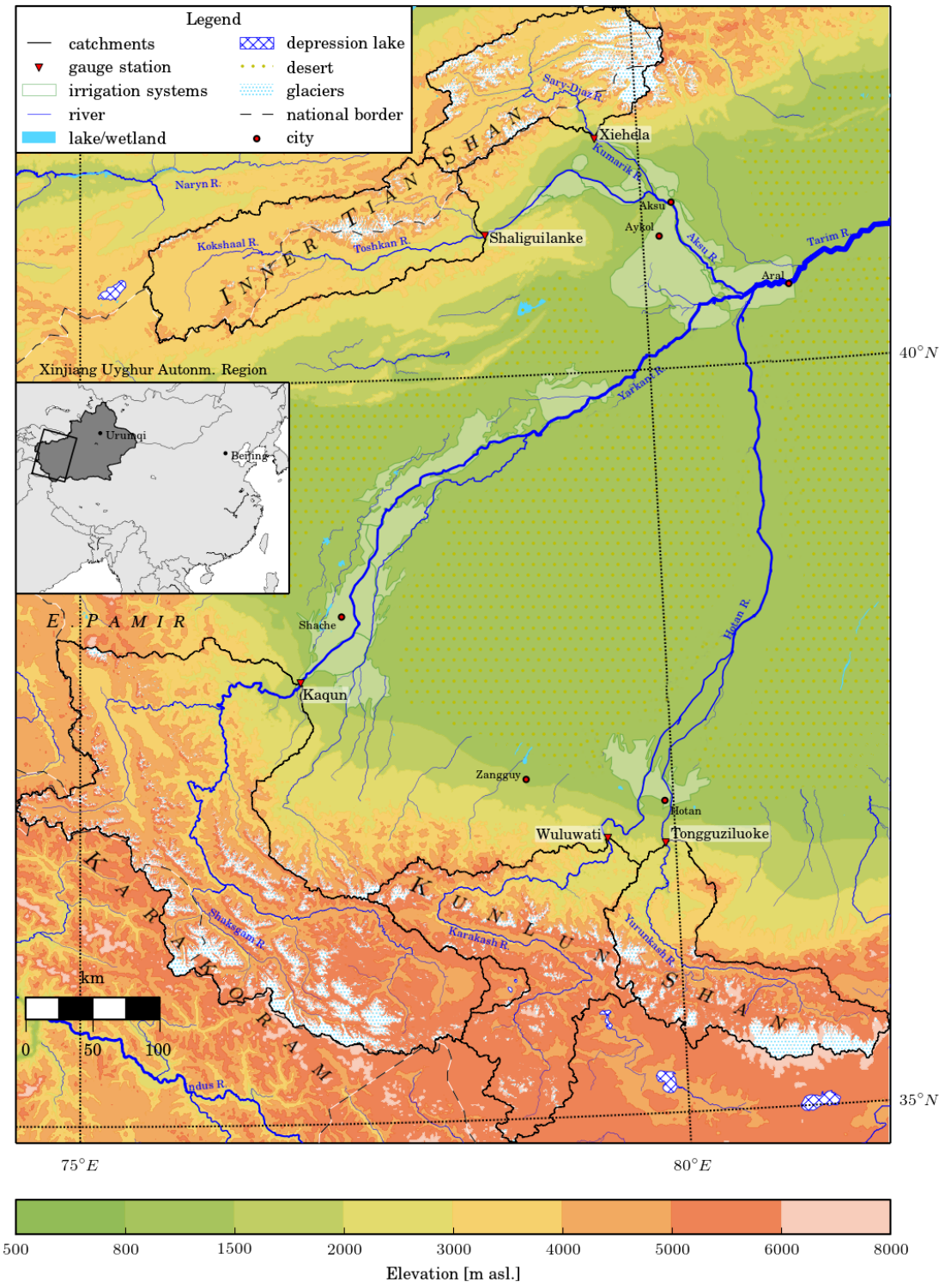

Figure 1 Map of the five considered catchments (their names marked by a white shade) that supply the vast majority of discharge to the Tarim River. Wortmann et al., 2018 © American Meteorological Society. Used with permission.

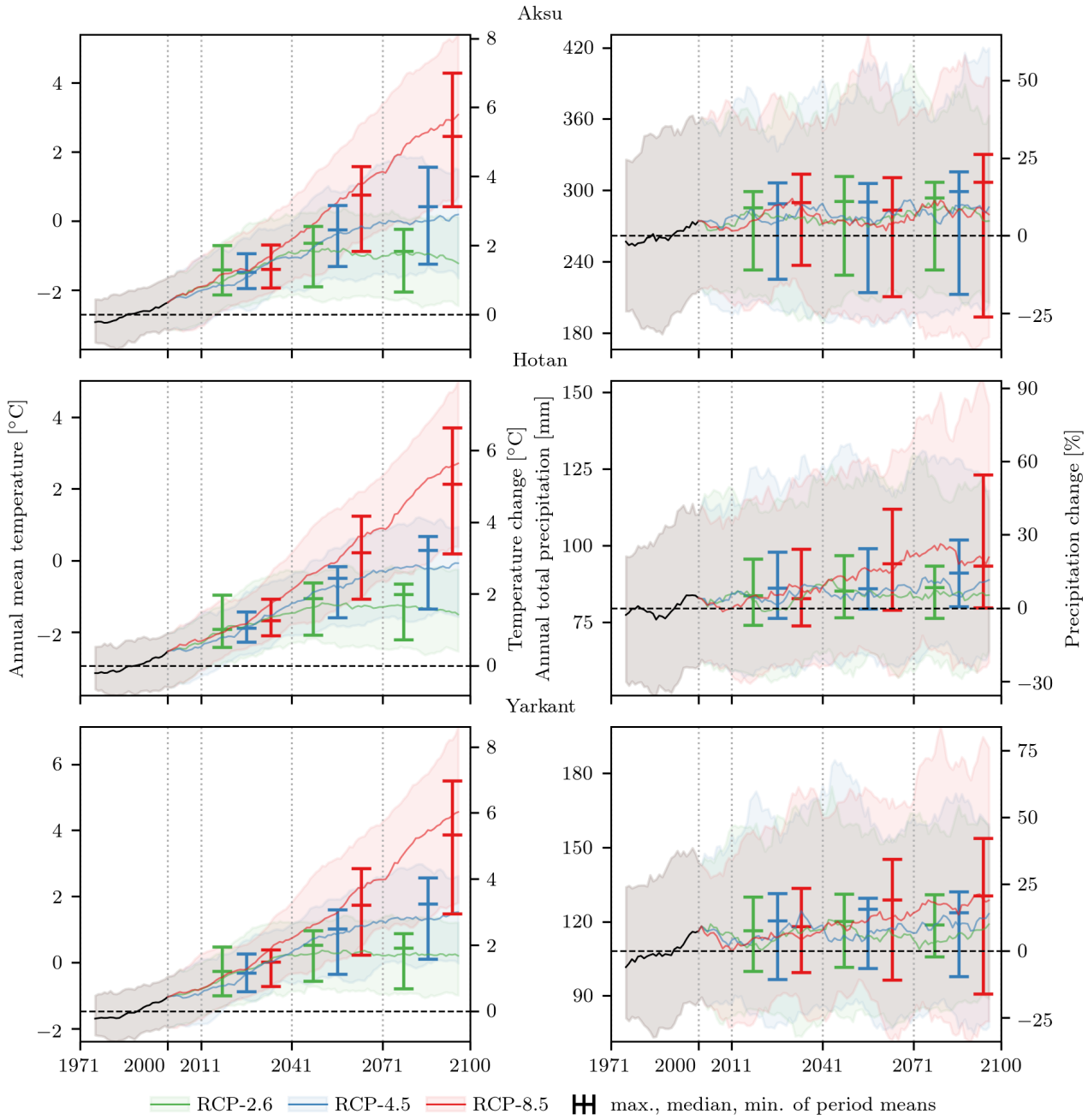

Figure 2 Climate change scenarios for the Tarim headwaters for the 21st century, including the reference period (1971–2000). Ensemble maximum, median and minimum values are shown as 10-year running means and signals averaged over the near (2011-40), medium (2041-70) and far (2071-2100) future. Absolute values are given in the left vertical axis and changes relative to the reference period along the right axis. Note that these are bias-adjusted GCM results without the static precipitation bias correction applied by the glacio-hydrological models. Monthly regimes of mean temperature, precipitation and snow fraction for all periods, scenarios and catchments are provided in Figure A4-A6 in the Annex.

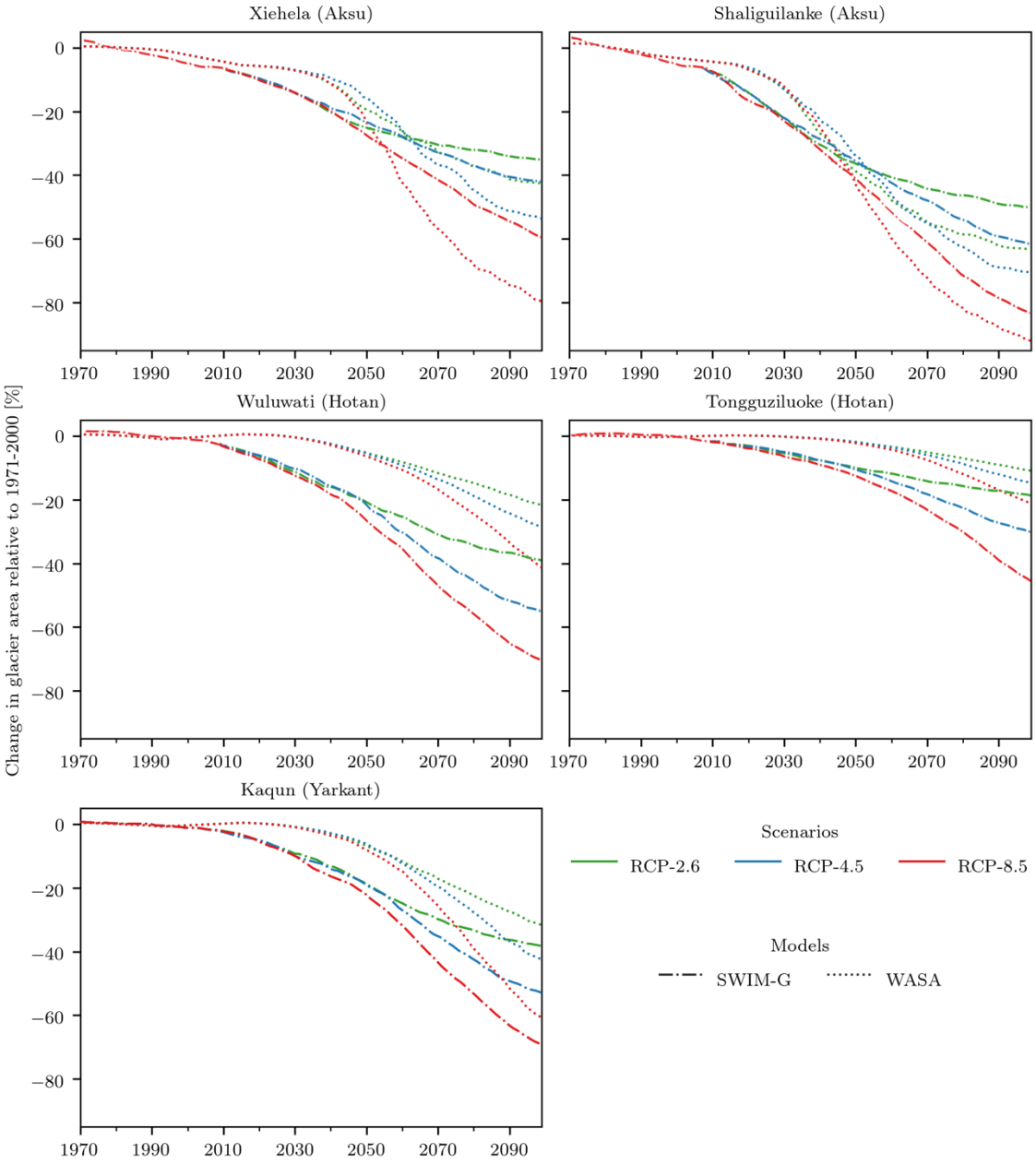

Figure 3 Simulated glacier area changes relative to mean area in the reference period (1971-2000) over the reference and scenario periods for the three RCP scenarios and the five catchments (indicated by their outlet station and main Tarim headwater river). Median values are computed over the climate model ensemble. Period mean values including ensemble standard deviations are provided in Table A4 in the Annex.

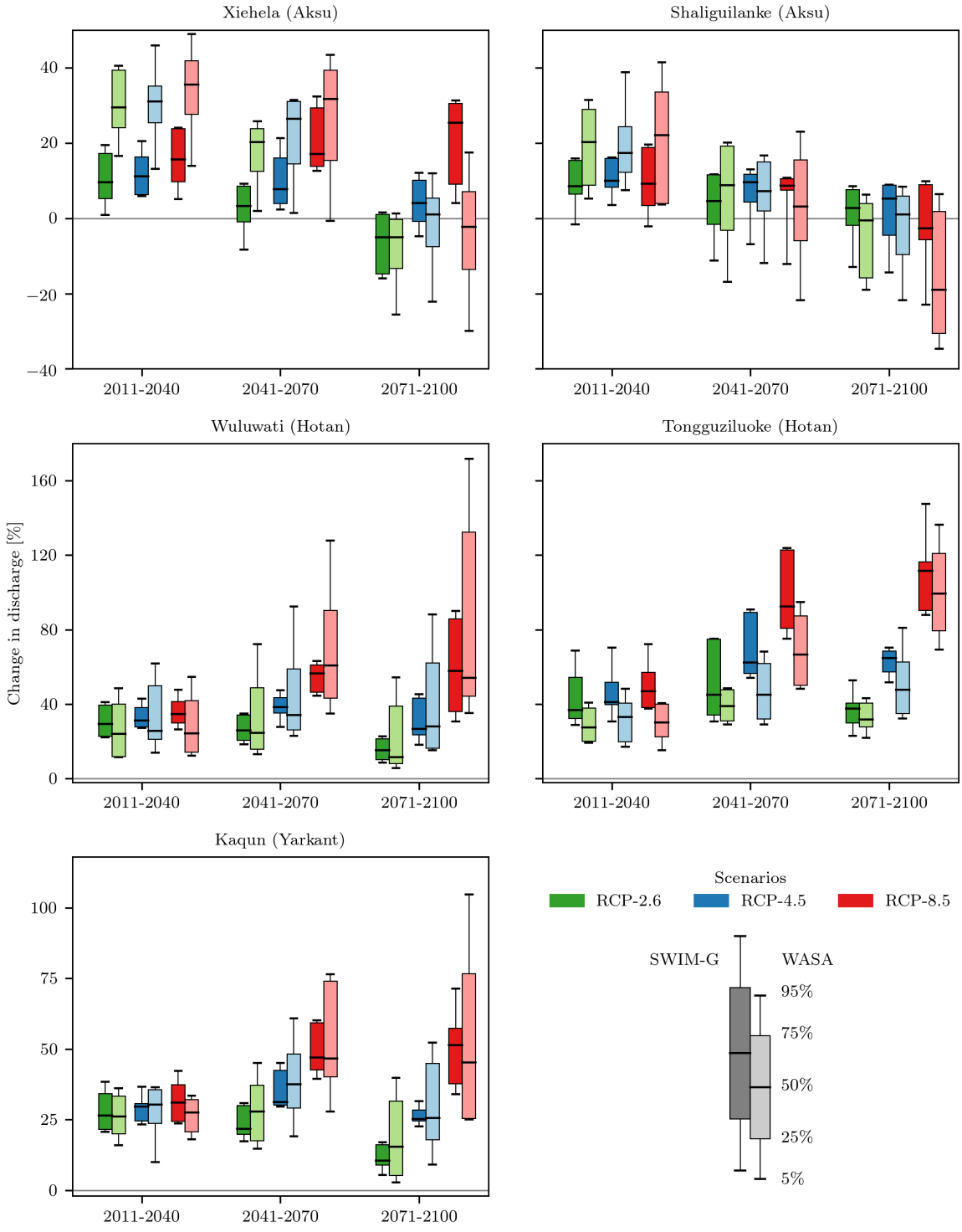

Figure 4 Projected future changes in annual mean discharge simulated by SWIM-G and WASA. Changes are relative to the baseline period 1971–2000.

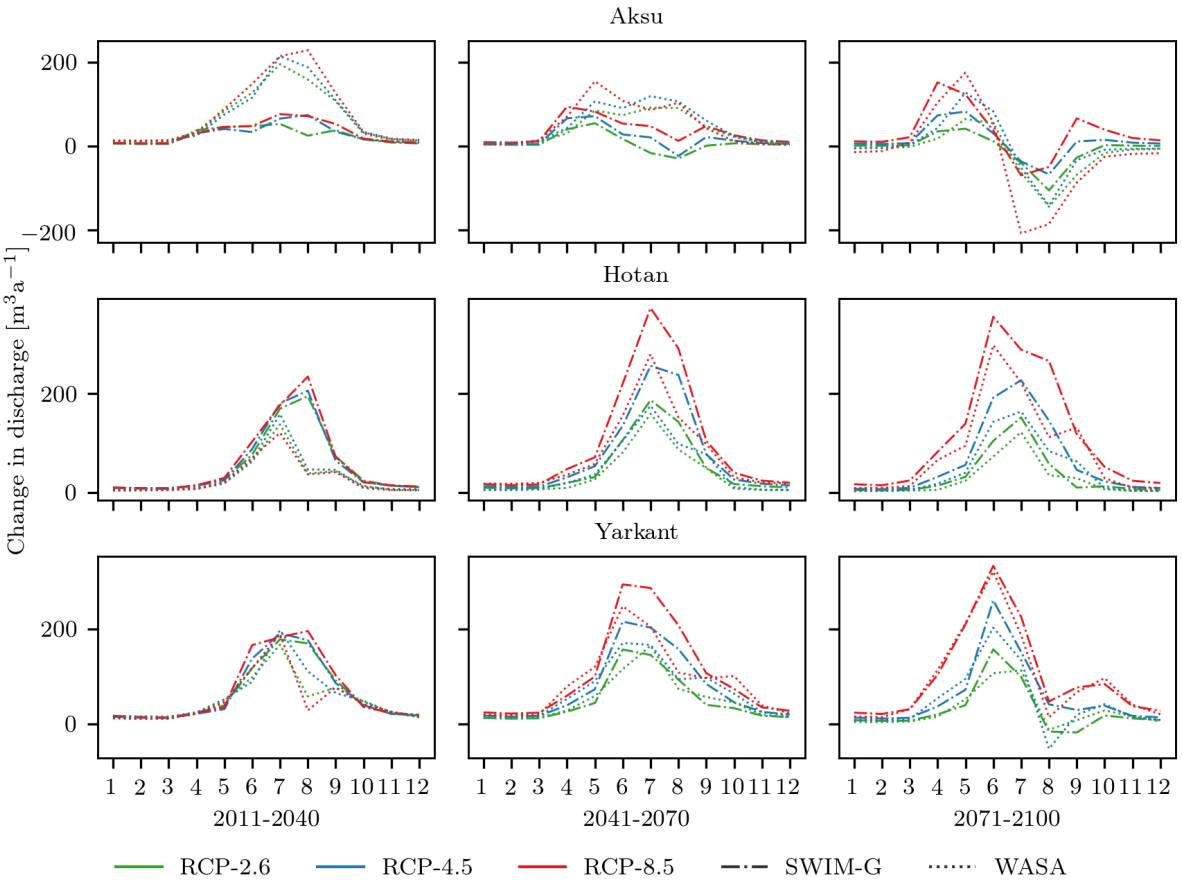

Figure 5 Absolute regime changes in the three main headwaters of the Tarim River (sum of both headwaters in the Aksu and Hotan). The ensemble median is shown for each scenario and glaciohydrological model. Rather than relative changes for each month in comparison with the reference period, the absolute monthly changes are shown to account for the highly seasonal flows.

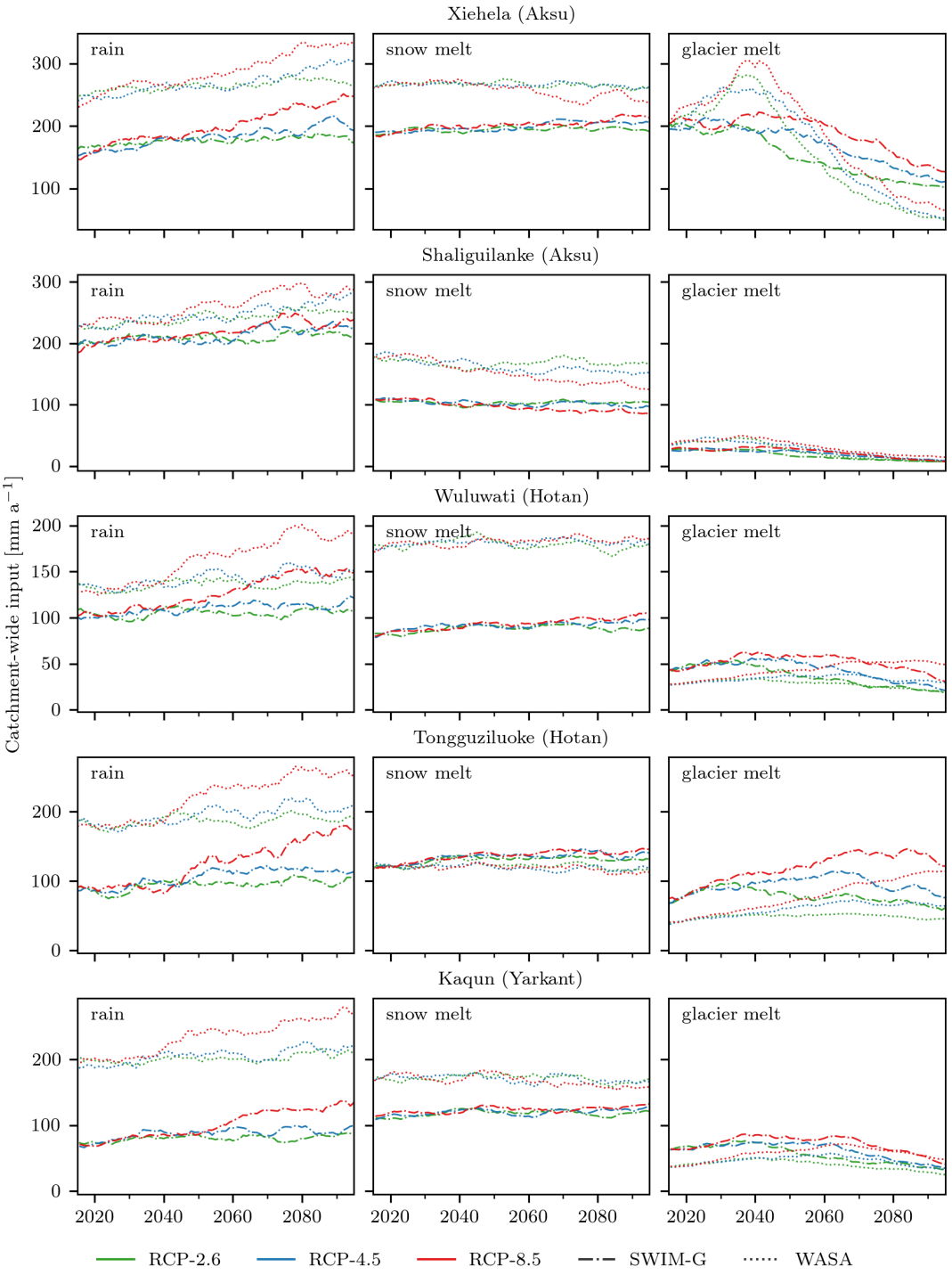

Figure 6 Projected glacier melt, snow melt and rain (absolute input values in mm a^{-1} distributed over the catchment areas). 10-year running mean values of the ensemble median for both SWIM-G and WASA are shown.